

# Dynamics of the Magnetoviscous Instability

Tanim Islam<sup>1</sup> & Steven Balbus<sup>1,2</sup>

## ABSTRACT

In dilute astrophysical plasmas, the collisional mean free path of a particle can exceed its Larmor radius. Under these conditions, the thermal conductivity and viscosity of the plasma can be dramatically altered. This alteration allows outwardly decreasing angular velocity or temperature gradients to become strongly destabilizing. This paper generalizes an earlier, simple analysis of the viscosity instability, by including the dynamical effects of magnetic field line tension. Such effects lower the growth rates found in the absence of such tension, but still allow growth rates in excess of the maximum of the standard magnetorotational instability. We find very good quantitative agreement with more complex kinetic treatments of the same process. The combination of large growth rates and large magnetic Prandtl number suggest that protogalactic disks are powerful dynamos.

*Subject headings:* accretion, accretion disks; magnetic fields; MHD; instabilities; galaxies: magnetic fields.

## 1. Introduction

Magnetic fields, even when highly subthermal, turn free energy gradients in sufficiently ionized fluids into sources of instability. There are important astrophysical consequences of this result: by the magnetorotational instability (MRI; Balbus & Hawley 1991), accretion disks become turbulent when angular velocity  $\Omega$ , rather than angular momentum  $\Omega R^2$ , decreases outward, and by the magnetothermal instability (MTI; Balbus 2001), dilute, stratified plasmas are destabilized when temperature rather than entropy decreases upwards.

---

<sup>1</sup>Department of Astronomy, P.O. Box 3818, University of Virginia, Charlottesville, VA 22903; [tsi6a@virginia.edu](mailto:tsi6a@virginia.edu)

<sup>2</sup>Laboratoire de Radioastronomie, École Normale Supérieure, 24 rue Lhomond, 75231 Paris, France; [steve.balbus@lra.ens.fr](mailto:steve.balbus@lra.ens.fr)

Since it is easier to violate the free energy gradient criteria than the classical Rayleigh and Schwarzschild criteria, it is the former, when applicable, that are relevant to the behavior of their host systems.

The MRI is the best-known example of a free-energy gradient instability, and has by now been extensively studied. Recently, however, it has been noted that purely viscous effects in a dilute MHD fluid can also lead to accretion disk turbulence, even if the  $\mathbf{J} \times \mathbf{B}$  Lorentz term ( $\mathbf{J}$  is the current density and  $\mathbf{B}$  is the magnetic density) is negligible (Balbus 2004; see Quataert et al. 2002 and Sharma et al. 2003 for plasma kinetic treatments). This is because there is a large parameter domain in which the ion Larmor radius is very small compared with fluid length scales (bounding the field strength from below), yet the magnetic field contribution to fluid stresses is tiny (bounding the field strength from above). If the plasma in question is sufficiently dilute, the ion cyclotron period is much smaller than the ion-ion collision time. Under these circumstances, the viscous stress tensor is highly anisotropic, and dominated by its diagonal terms (6). These circumstances are similar to those of anisotropic thermal conduction. In the MTI, heat, borne by the electrons, flows only along the magnetic lines of force. In the viscous case, it is of course angular momentum flow that is restricted. In both cases, fluid attributes that are ordinarily responsible for stabilizing dissipation (thermal conduction, viscosity) become active agents of destabilization, a remarkable turn of events.

The cause of the instability is essentially the same in both cases. Perturbed magnetic field lines, initially isothermal (isorotational), are stretched along the direction of the background temperature (angular velocity) gradient. This allows heat (angular momentum) to flow from one fluid element to another. The elements then move yet farther apart, the field lines become more aligned with the background gradient, and the process runs away. The magnetothermal instability has been followed calculated far into the nonlinear regime, in which vigorous convection has developed (Parrish & Stone 2005).

Neglect of the fluid  $\mathbf{J} \times \mathbf{B}$  force in the magnetoviscous calculation of Balbus (2004), while enabling a point of principle to be made more transparently, ultimately restricts the domain of validity. Magnetic stresses are an important complication, acting as both a stabilizing and destabilizing agent. To understand the true nature of this instability in an astrophysical context, it is desirable to pursue a more general approach, and this is the primary motivation of the current paper.

In §2, we discuss the physical parameter regime in which this work is expected to apply, and present the formalism by which the components of the magnetic viscosity may be calculated. In §3, we formulate the problem and obtain the dispersion relation of interest. Characteristic growth rates are determined, and the physical regime reexamined for self-consistency. In §4, we present a discussion relating our work to a more complex plasma kinetic

treatment, and touch upon some astrophysical implications. Finally, in §V, we summarize our conclusions.

## 2. Preliminaries

### 2.1. Parameters

The magnetoviscous instability finds its natural venue in protogalactic disks and halos, as well as in very low density accretion flows, of which the Galactic center is the prototype (Melia & Falcke 2000). These systems are characterized by subthermal magnetic fields in collisionless plasmas and ohmic diffusion coefficients small relative to the viscous diffusion coefficient. Let  $\omega_{ci}$  be the ion cyclotron frequency, and  $\tau_i$  the ion-ion collision time:

$$\tau_i \simeq 5.91 \times 10^5 \left( \frac{20}{n \ln \Lambda} \right) T_4^{3/2} \text{ s}, \quad (1)$$

where  $n$  is the proton density in  $\text{cm}^{-3}$ ,  $T_4$  the ion kinetic temperature in units of  $10^4$  K and  $\ln \Lambda$  is Coulomb logarithm. We shall work in the asymptotic domain

$$\omega_{ci}\tau_i = \left( \frac{1.09 \times 10^5}{n} \right) \frac{T_4^{3/2} B_{\mu G}}{\ln \Lambda} \gg 1, \quad (2)$$

where  $B_{\mu G}$  is the magnetic field strength in microgauss. With  $n \lesssim 1$  and  $T_4 \gtrsim 1$ , even very weak fields can be accommodated by this regime. On the other hand, we shall also assume that the Reynolds number is large, which requires

$$\Omega\tau_i \ll 1, \quad (3)$$

where  $\Omega$  is the disk rotational frequency. The collision frequency  $1/\tau_i$  is therefore much larger than an orbital frequency, but much smaller than the cyclotron frequency. Finally, let us note the Prandtl number ratio of the viscosity to ohmic resistivity (Balbus & Hawley 1998):

$$\mathcal{P} = \left( \frac{T}{10^4} \right)^4 \left( \frac{6.5 \times 10^{10}}{n} \right) \left( \frac{20}{\ln \Lambda} \right)^2. \quad (4)$$

We shall assume  $\mathcal{P} \gg 1$ . The Spitzer (1962) viscosity for a hydrogenic plasma is:

$$\eta \simeq 1.1 \times 10^{-16} T^{5/2} \left( \frac{20}{\ln \Lambda} \right) \text{ g cm}^{-1} \text{ s}^{-1}. \quad (5)$$

(Applications to low luminosity black hole accretion should use a value of  $\ln \Lambda$  closer to 30.) Finally, for future reference, we use the standard plasma  $\beta$  parameter to represent the ratio

of the gas to magnetic pressures:

$$\beta = \frac{8\pi P}{B^2}. \quad (6)$$

It is helpful to have representative physical parameters at hand, even if they are very crude. For protogalactic disks, densities could range from  $10^{-2}$  to 1 particle per  $\text{cm}^3$ ; temperatures from  $10^4$  to  $10^6$  K. For radiatively inefficient black hole accretion flows, a typical density might be  $10^8 \text{ cm}^{-3}$ , but the range of interest should be thought of as perhaps  $10^5 - 10^{10}$ . The ion and electron temperatures seem to be very different in these flows: the ions ought to be virialized at  $T \sim 10^{12}$  K, whereas the electrons are thought to be  $\lesssim 10^{10}$  K (Narayan, Mahadevan, & Quataert 1998 for a review). In a forthcoming paper, we shall discuss a possible reason for this two temperature structure based on the MTI.

## 2.2. Magnetic Viscosity

A convenient formalism for the viscous stress tensor in the presence of a magnetic field is presented in Balbus (2004), and shall quote the results here for reference, referring the reader to this paper for further details.

Our fundamental coordinate system for the disk will be a standard cylindrical system: radius  $R$ , azimuth  $\phi$ , and axial variable  $Z$ . Define now a local Cartesian system, determined by the magnetic field. We denote these axes by subscript  $b$ .  $Z_b$  points along the local direction of the magnetic field,  $X_b$  and  $Y_b$  may be any axes orthogonal to one another as well as to the  $Z_b$  direction. Following Braginskii (1965), the  $Z_b Z_b$  component of the viscous stress  $\sigma_{Z_b Z_b}$  is unaffected by the presence of the field. It is given by (Balbus 2004):

$$\sigma_{Z_b Z_b} = -2\eta [(\mathbf{b} \cdot \nabla)\mathbf{v}] \cdot \mathbf{b}, \quad (7)$$

where  $\mathbf{v}$  the local velocity field, and  $\mathbf{b}$  is a unit vector in the direction of the magnetic field. The other diagonal components of the traceless viscous stress are

$$\sigma_{X_b X_b} = \sigma_{Y_b Y_b} = -\sigma_{Z_b Z_b}/2. \quad (8)$$

To find the components of the magnetized viscous stress tensor in any other local Cartesian frame, the transformation law may be written

$$\sigma_{ij} = \sum_{i_b, j_b} (\mathbf{i} \cdot \mathbf{i}_b) (\mathbf{j} \cdot \mathbf{j}_b) \sigma_{i_b j_b}, \quad (9)$$

where once again the  $b$  subscript denotes the magnetic field frame and bold face quantities are unit vectors of the indicated component. Using equation (8) for the nonvanishing diagonal

stress tensor components in the field frame, we obtain

$$\sigma_{ij} = \sigma_{Z_b Z_b} \left[ (\mathbf{i} \cdot \mathbf{Z}_b)(\mathbf{j} \cdot \mathbf{Z}_b) - \frac{1}{2}(\mathbf{i} \cdot \mathbf{Y}_b)(\mathbf{j} \cdot \mathbf{Y}_b) - \frac{1}{2}(\mathbf{i} \cdot \mathbf{X}_b)(\mathbf{j} \cdot \mathbf{X}_b) \right]. \quad (10)$$

Once  $\sigma_{Z_b Z_b}$  is determined in the magnetic field frame,  $\sigma_{ij}$  may be calculated in any frame.

### 3. Formulation of the Problem

#### 3.1. Braginskii Stress

We consider the stability of a disk under the influence of a weak magnetic field. As in standard MRI analyses, we assume that the field is sufficiently weak that it has no effect on the equilibrium state, but that magnetic tension is important for the behavior of local WKB perturbations. The fundamental fluid equations used here are mass conservation,

$$\frac{\partial \rho}{\partial t} + \nabla \cdot (\rho \mathbf{v}) = 0, \quad (11)$$

the equation of motion,

$$\rho \left( \frac{\partial}{\partial t} + \mathbf{v} \cdot \nabla \right) \mathbf{v} = -\nabla \left( P + \frac{B^2}{8\pi} \right) + \frac{1}{4\pi} (\mathbf{B} \cdot \nabla) \mathbf{B} - \rho \nabla \Phi - \frac{\partial \sigma_{ij}}{\partial x_j}, \quad (12)$$

and the induction equation of ideal MHD,

$$\frac{\partial \mathbf{B}}{\partial t} = \nabla \times (\mathbf{v} \times \mathbf{B}). \quad (13)$$

$\Phi$  represents an external gravitational potential and the other symbols have their usual meanings; the viscous stress tensor  $\sigma_{ij}$  is given by equation (10).

The equilibrium state is a differentially rotating disk. As stated above, we work in a standard cylindrical coordinate system,  $R, \phi, Z$ . The angular velocity is  $\Omega(R)$ , and we shall restrict ourselves to a local analysis at the midplane. Thus, we may ignore buoyant forces.

In the equilibrium state, it is assumed that  $\sigma_{ij} = 0$ ; it will be shown that this is in general not a stable configuration. The initial magnetic field lines are spooled around cylinders, unaffected by the shear.

We consider next small departures from the equilibrium flow. Linearly perturbed quantities are denoted by  $\delta \mathbf{v}, \delta \sigma_{ij}$ , etc. We work in the local WKB limit, with the space-time dependence of all perturbed quantities given by  $\exp(\gamma t + i \mathbf{k} \cdot \mathbf{r})$ . Thus,  $\gamma$  is a growth or decay rate if it is real, and an angular frequency if it is imaginary.

To evaluate  $\delta\sigma_{ij}$  we follow Balbus (2004). Since  $\sigma_{ij}$  vanishes in the equilibrium state, it follows from equation (10) that

$$\delta\sigma_{ij} = \delta\sigma_{Z_b Z_b} \left[ (\mathbf{i} \cdot \mathbf{Z}_b)(\mathbf{j} \cdot \mathbf{Z}_b) - \frac{1}{2}(\mathbf{i} \cdot \mathbf{Y}_b)(\mathbf{j} \cdot \mathbf{Y}_b) - \frac{1}{2}(\mathbf{i} \cdot \mathbf{X}_b)(\mathbf{j} \cdot \mathbf{X}_b) \right]. \quad (14)$$

The geometry of the equilibrium field is defined by

$$\mathbf{b} = \cos \chi \hat{\boldsymbol{\phi}} + \sin \chi \hat{\mathbf{Z}}. \quad (15)$$

$\hat{\boldsymbol{\phi}}$ ,  $\hat{\mathbf{Z}}$ , and  $\hat{\mathbf{R}}$  (used below) are unit vectors in the indicated cylindrical directions, and  $\chi$  is the angle between the magnetic field and the  $\phi$  axis. The local magnetic field axes are chosen to be

$$\mathbf{Z}_b = \mathbf{b} = \cos \chi \hat{\boldsymbol{\phi}} + \sin \chi \hat{\mathbf{Z}}, \quad (16)$$

$$\mathbf{X}_b = \hat{\mathbf{R}} \times \mathbf{Z}_b = -\sin \chi \hat{\boldsymbol{\phi}} + \cos \chi \hat{\mathbf{Z}}, \quad (17)$$

and

$$\mathbf{Y}_b = \hat{\mathbf{R}}. \quad (18)$$

See fig. 2.

The diagonal elements of  $\delta\sigma_{ij}$  are found to be

$$\delta\sigma_{RR} = -\frac{1}{2}\delta\sigma_{Z_b Z_b}, \quad \delta\sigma_{\phi\phi} = \left( \cos^2 \chi - \frac{\sin^2 \chi}{2} \right) \delta\sigma_{Z_b Z_b}, \quad \delta\sigma_{ZZ} = \left( \sin^2 \chi - \frac{\cos^2 \chi}{2} \right) \delta\sigma_{Z_b Z_b}, \quad (19)$$

and the off-diagonal elements are

$$\delta\sigma_{\phi Z} = \delta\sigma_{Z\phi} = \frac{3}{2} \cos \chi \sin \chi \delta\sigma_{Z_b Z_b}. \quad (20)$$

Finally, we evaluate  $\delta\sigma_{Z_b Z_b}$  from its vector-invariant form (7),

$$\delta\sigma_{Z_b Z_b} = -2\eta \left( [(\boldsymbol{\delta}\mathbf{b} \cdot \boldsymbol{\nabla})\mathbf{v}] \cdot \mathbf{b} + [(\mathbf{b} \cdot \boldsymbol{\nabla})\boldsymbol{\delta}\mathbf{v}] \cdot \mathbf{b} + [(\mathbf{b} \cdot \boldsymbol{\nabla})\mathbf{v}] \cdot \boldsymbol{\delta}\mathbf{b} \right). \quad (21)$$

Using  $\mathbf{v} = R\Omega\hat{\boldsymbol{\phi}}$  and equation (16), we obtain

$$\delta\sigma_{Z_b Z_b} = -2\eta \left[ \delta b_R \frac{d\Omega}{d \ln R} \cos \chi + i(\mathbf{k} \cdot \mathbf{b})(\mathbf{b} \cdot \boldsymbol{\delta}\mathbf{v}) \right]. \quad (22)$$

### 3.2. Linearized Equations

The linearized dynamical equations are

$$\mathbf{k} \cdot \delta \mathbf{v} = 0, \quad (23)$$

$$\gamma \delta v_R - 2\Omega \delta v_\phi + \frac{ik_R}{\rho} \left( \delta P - \frac{\delta \sigma_{Z_b Z_b}}{2} + \frac{\mathbf{B} \cdot \delta \mathbf{B}}{4\pi} \right) - \frac{ik_Z B_Z \sin \chi}{4\pi \rho} \delta B_R = 0, \quad (24)$$

$$\gamma \delta v_\phi + \frac{\kappa^2}{2\Omega} \delta v_R + i \frac{3k_Z}{2\rho} \sin \chi \cos \chi \delta \sigma_{Z_b Z_b} - \frac{ik_Z B_Z \sin \chi}{4\pi \rho} \delta B_\phi = 0, \quad (25)$$

(Here,  $\kappa^2$  is the square of the epicyclic frequency,  $\kappa^2 = 4\Omega^2 + d\Omega^2/d \ln R$ .)

$$\gamma \delta v_Z + \frac{ik_Z}{\rho} \left[ \delta P + \left( \sin^2 \theta - \frac{\cos^2 \theta}{2} \right) \delta \sigma_{Z_b Z_b} \right] - \frac{ik_Z B_Z \sin \chi}{4\pi \rho} \delta B_Z = 0. \quad (26)$$

The induction equations are

$$\gamma \delta B_R - ik_Z B_Z \sin \chi \delta v_R = 0, \quad (27)$$

$$\gamma \delta B_\phi - \delta B_R \frac{d\Omega}{d \ln R} - k_Z B_Z \sin \chi \delta v_\phi = 0, \quad (28)$$

$$\gamma \delta B_Z - ik_Z B_Z \sin \chi \delta v_Z = 0. \quad (29)$$

Finally, we recast equation (22) for the all-important  $Z_b Z_b$  stress component in a more convenient form,

$$\delta \sigma_{Z_b Z_b} = -2\eta ik_Z \sin \chi \left[ \cos \chi \left( \frac{\delta v_R}{\gamma} \frac{d\Omega}{d \ln R} + \delta v_\phi \right) + \sin \chi \delta v_Z \right]. \quad (30)$$

### 3.3. Dispersion Relation

The linearized equations lead, after straightforward but somewhat tedious algebra, to a dispersion relation that blends the properties of the magnetorotational and magnetoviscous instabilities:

$$\begin{aligned} & \frac{k^2}{k_Z^2} \gamma^4 + 3\eta_V \gamma^3 \sin^2 \chi k_\perp^2 (k_R^2 + k_Z \cos^2 \chi) + \gamma^2 \left( \kappa^2 + 2 \frac{k^2}{k_Z^2} (\mathbf{k} \cdot \mathbf{v}_A)^2 \right) + \\ & + 3\eta_V \gamma \sin^2 \chi \left[ (\mathbf{k} \cdot \mathbf{v}_A)^2 k_\perp^2 + k_Z^2 \cos^2 \chi \frac{d\Omega^2}{d \ln R} \right] + (\mathbf{k} \cdot \mathbf{v}_A)^2 \left[ \frac{k^2}{k_Z^2} (\mathbf{k} \cdot \mathbf{v}_A)^2 + \frac{d\Omega^2}{d \ln R} \right] = 0, \end{aligned} \quad (31)$$

where  $k_{\perp}^2 = k_R^2 + k_Z^2 \cos^2 \chi$  is the square of the component of the wavenumber perpendicular to  $\mathbf{b}$ , and  $\eta_V$  is the kinematic viscosity  $\eta/\rho$ . We note that in the limit  $\eta_V \rightarrow 0$  the standard MRI dispersion relation is recovered, while in the limit  $\mathbf{k} \cdot \mathbf{v}_A \rightarrow 0$ , the magnetoviscous dispersion relation of Balbus (2004) emerges (taking also the limit  $k_R = 0$ ). Unstable modes are present if  $d\Omega^2/dR < 0$ , as expected.

To evaluate the growth rates associated with the dynamical magnetoviscous instability, we proceed as follows. First, we set  $k_R = 0$ , which corresponds to the most rapidly growing modes, and simplifies the calculation. Second, we calculate all rates ( $\gamma$ ,  $\mathbf{k} \cdot \mathbf{v}_A$ ,  $\kappa$ ,  $\eta_V k_{\perp}^2$ ) in units of  $\Omega$ . We introduce the notation

$$X \equiv (\mathbf{k} \cdot \mathbf{v}_A)^2/\Omega^2, \quad Y = 3\eta_V \sin^2 \chi k_{\perp}^2/\Omega, \quad \gamma' = \gamma/\Omega, \quad (32)$$

and restrict ourselves to the astrophysically interesting case of  $d\Omega^2/dR < 0$ . Our dispersion relation may then be rewritten as

$$Y = \frac{\gamma'^4 + \gamma'^2[(\kappa/\Omega)^2 + 2X] + X(X + d \ln \Omega^2/d \ln R)}{\gamma'(|d \ln \Omega^2/d \ln R| - X - \gamma'^2)}. \quad (33)$$

Triples of the form  $(X, Y, \gamma')$  are easily calculated by this formula, and contour plots of  $\gamma$  thereby generated. In fact, it is convenient to view the results in the  $Y/X$ ,  $X$  plane since the wavenumber is thereby removed from the ordinate, which becomes a normalized viscosity. The results are shown in figures 1 (Keplerian rotation profile) and 2 (galactic rotation profile). The maximum possible growth rate is

$$\gamma_{max}^2 = \left| \frac{d\Omega^2}{d \ln R} \right|. \quad (34)$$

as found by plasma kinetic treatments (Quataert et al. 2002; Sharma et al. 2003) and for the magnetoviscous instability (Balbus 2004). The effect of magnetic tension is to lower the maximum growth rate to somewhere between this value, and the MRI maximum rate of  $0.5|d\Omega/d \ln R|$ .

### 3.4. Physical Regime

Figures (1) and (2) show that magnetoviscous effects can significantly change the inviscid MRI growth rates in the parameter regime  $X \lesssim 1$ ,  $Y \gtrsim 1$ . Let us determine what sort of magnetic field strengths are implied by this condition in an environment representative of a protogalaxy. With  $\sin^2 \chi$  set equal to a half,

$$Y = \frac{1.5\eta_V k_{\perp}^2}{\Omega} = \frac{1.5\eta_V \Omega}{c_s^2} (k_{\perp} H)^2, \quad (35)$$

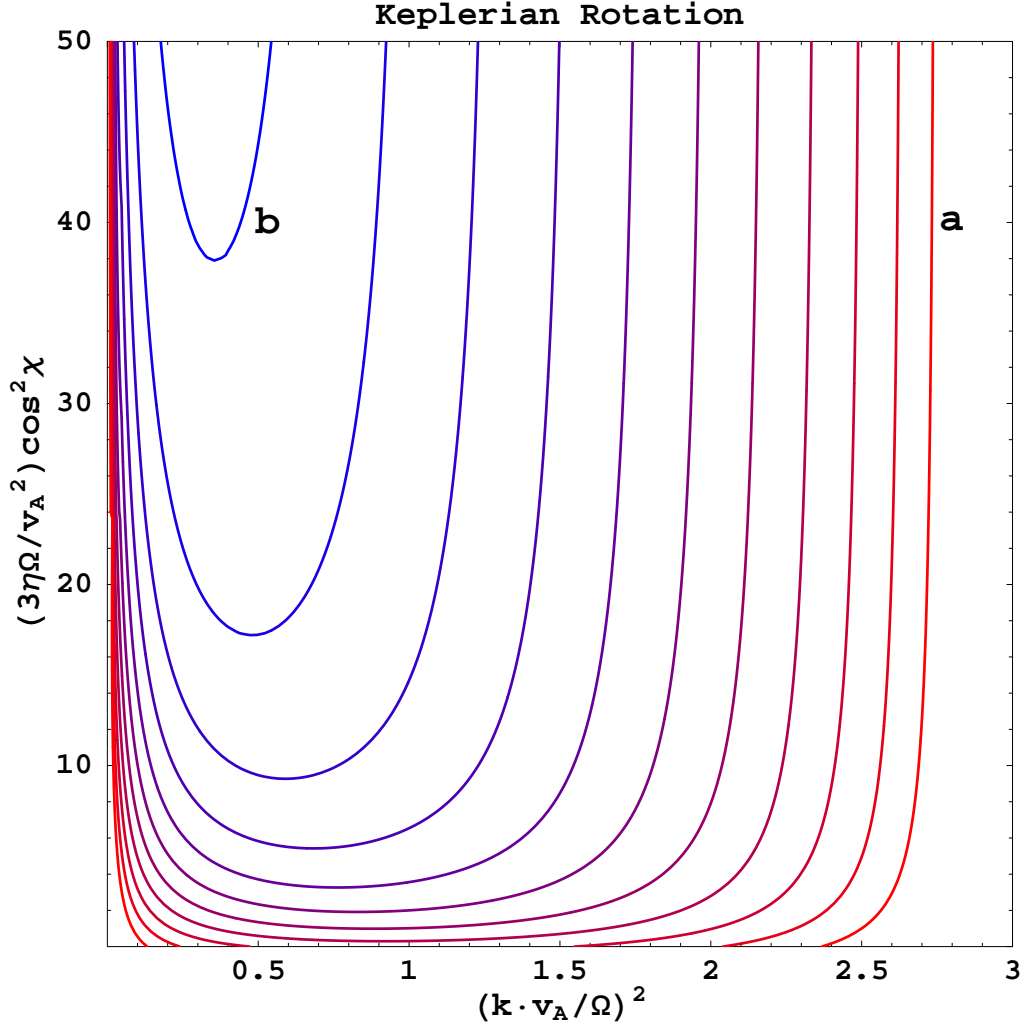


Fig. 1.— Contours of normalized growth rate  $\gamma/\Omega$  for a Keplerian rotation profile, as a function of normalized wavenumber  $(\mathbf{k} \cdot \mathbf{v}_A/\Omega)^2$  and normalized viscosity  $3\eta\Omega \cos^2 \chi/v_A^2$ . Contours run from  $\gamma = 0.5\Omega$  (contour a) to  $\gamma = 1.5\Omega$  (contour b) in steps of  $0.1\Omega$ . The maximum MRI growth rate is  $0.75\Omega$ .

where we have introduced the isothermal sound speed  $c_S$  and scale height  $H$  defined by  $H\Omega = c_S$ . Replacing  $\eta_V$  by  $\rho\eta$  and using equation (5), we find

$$Y = \frac{2.39 \times 10^{-8} T_4^{3/2} \Omega_{-14}}{n} (k_{\perp} H)^2, \quad (36)$$

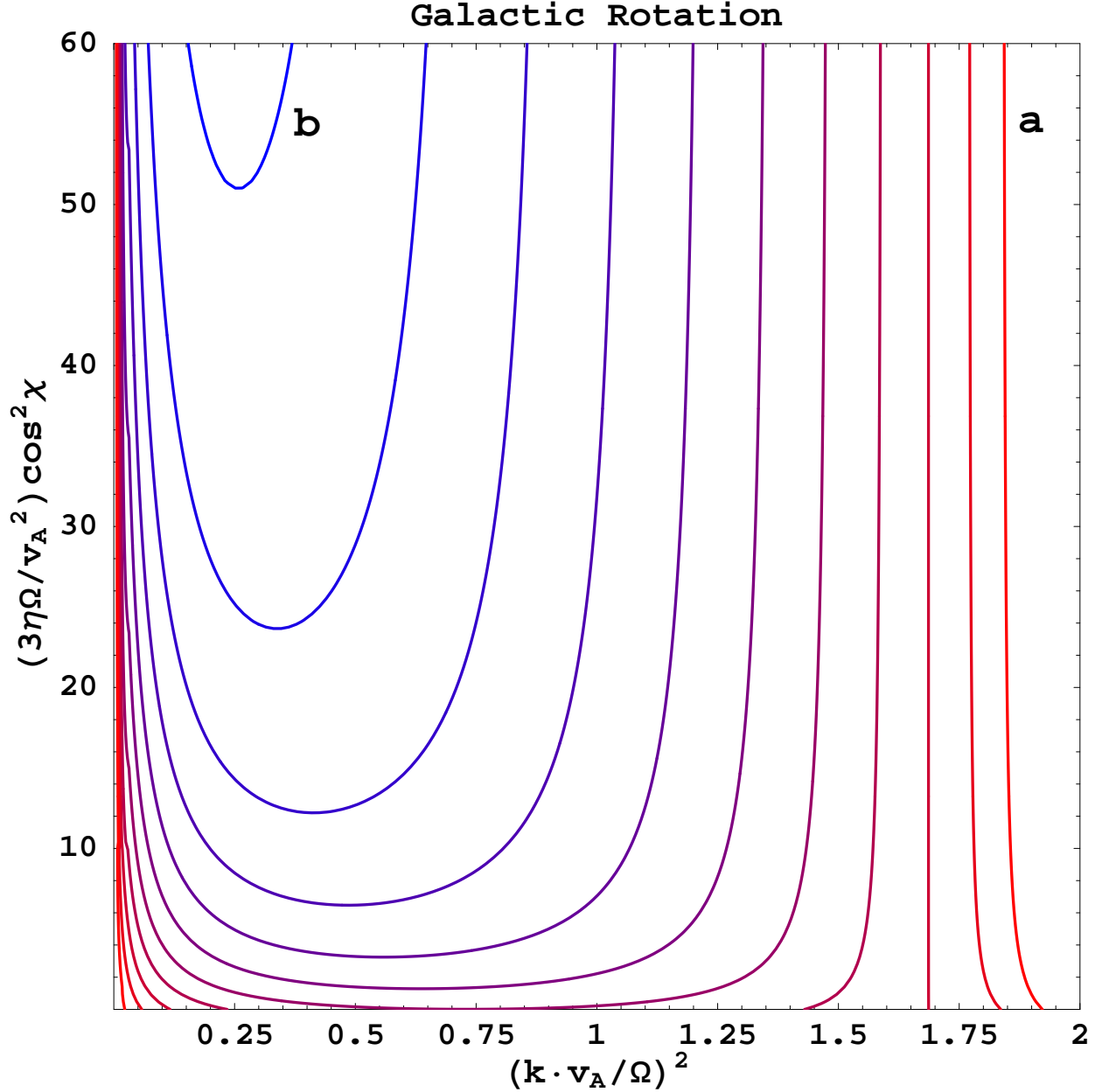


Fig. 2.— Contours of normalized growth rate  $\gamma/\Omega$  for a galactic rotation profile ( $\Omega \propto R^{-1}$ ), as a function of normalized wavenumber  $(\mathbf{k} \cdot \mathbf{v}_A/\Omega)^2$  and normalized viscosity  $3\eta\Omega \cos^2 \chi/v_A^2$ . Contours run from  $\gamma = 0.4\Omega$  (contour a) to  $\gamma = 1.2\Omega$  (contour b) in steps of  $0.08\Omega$ . The maximum MRI growth rate is  $0.5\Omega$ .

where  $T_4$  is the temperature in units of  $10^4\text{K}$ , and  $\Omega$  the angular rotation rate in units of  $10^{-14} \text{ rad s}^{-1}$ . In other words,

$$(k_{\perp}H)^2 \gtrsim 4.2 \times 10^7 \frac{nT_4^{-3/2}}{\Omega_{-14}}, \quad (37)$$

for viscous effects to be important. On the other hand,  $X \lesssim 1$  for the growth rates to be significantly enhanced. Since

$$X = \frac{k_Z^2 v_A^2}{\Omega^2} = (k_Z H)^2 \frac{v_A^2}{c_S^2} = 2 \frac{(k_Z H)^2}{\beta}, \quad (38)$$

we find that

$$\beta \gtrsim 2k_Z^2 H^2 \gtrsim 8.4 \times 10^7 \left( \frac{nT_4^{-3/2}}{\Omega_{-14}} \right) \quad (39)$$

(ignoring the distinction between  $k_Z$  and  $k_\perp$ .) This translates to a magnetic field strength of

$$B \lesssim 6.5 \times 10^{-10} T_4^{5/4} \Omega_{-14}^{1/2} \text{ G}. \quad (40)$$

This is of the order of the strength of the seed field estimated in Balbus (2004), obtained by diluting stellar surface magnetic fields of strength  $\sim 0.1$  G over parsec scales. For applications to inefficiently radiating black hole accretion flows, the permissible  $\beta$  parameter regime can extend to values near unity.

#### 4. Comparison with Plasma Kinetic Treatment

Anisotropic stresses in the presence of a magnetic field may be calculated from a moment expansion of the collisionless Boltzmann equation using a formalism developed by Kulsrud (1983). (In the absence of a heat flux, this reduces to a double-adiabatic equation of state first derived by Chew et al. [1956].) This approach has been applied to the MRI in the fully collisionless regime (Quataert et al. 2002) and the collisional regime (Sharma et al. 2003; see also Snyder, Hammett & Dorland 1997). In the fully collisional limit, Sharma et al. recover the MRI, as do we in the limit  $\eta_V \rightarrow 0$ . The fluid and plasma kinetic treatments are markedly different in their level of complexity, and a quantitative comparison of their findings is therefore of interest. This is shown in figures 3 and 4. We have adopted the fiducial case of Sharma et al. (2003). This corresponds to  $\chi = 45^\circ$ ,  $\beta_Z = 8\pi P/B_Z^2 = 10^4$ . Choosing values for  $\mathbf{k} \cdot \mathbf{v}_A/\Omega$  and  $\nu/\Omega$ , where  $\nu$  is the ion self-collision frequency, then allows our  $X$  and  $Y$  parameters to be determined, once use is made of the Spitzer viscosity (5). The figures show the growth rates as a function of  $\mathbf{k} \cdot \mathbf{v}_A/\Omega$  for several different values of  $\nu/\Omega$ . In general the two approaches are in excellent agreement (growth rates agree to within  $\sim 5$ ), with significant disparity coming only in the completely collisionless regime (infinite viscosity). This is not unexpected, since it corresponds to the complete breakdown of the fluid regime. What is remarkable is how well the relatively simple fluid treatment performs. The savings of effort is the greater the more complex the problem. For example,

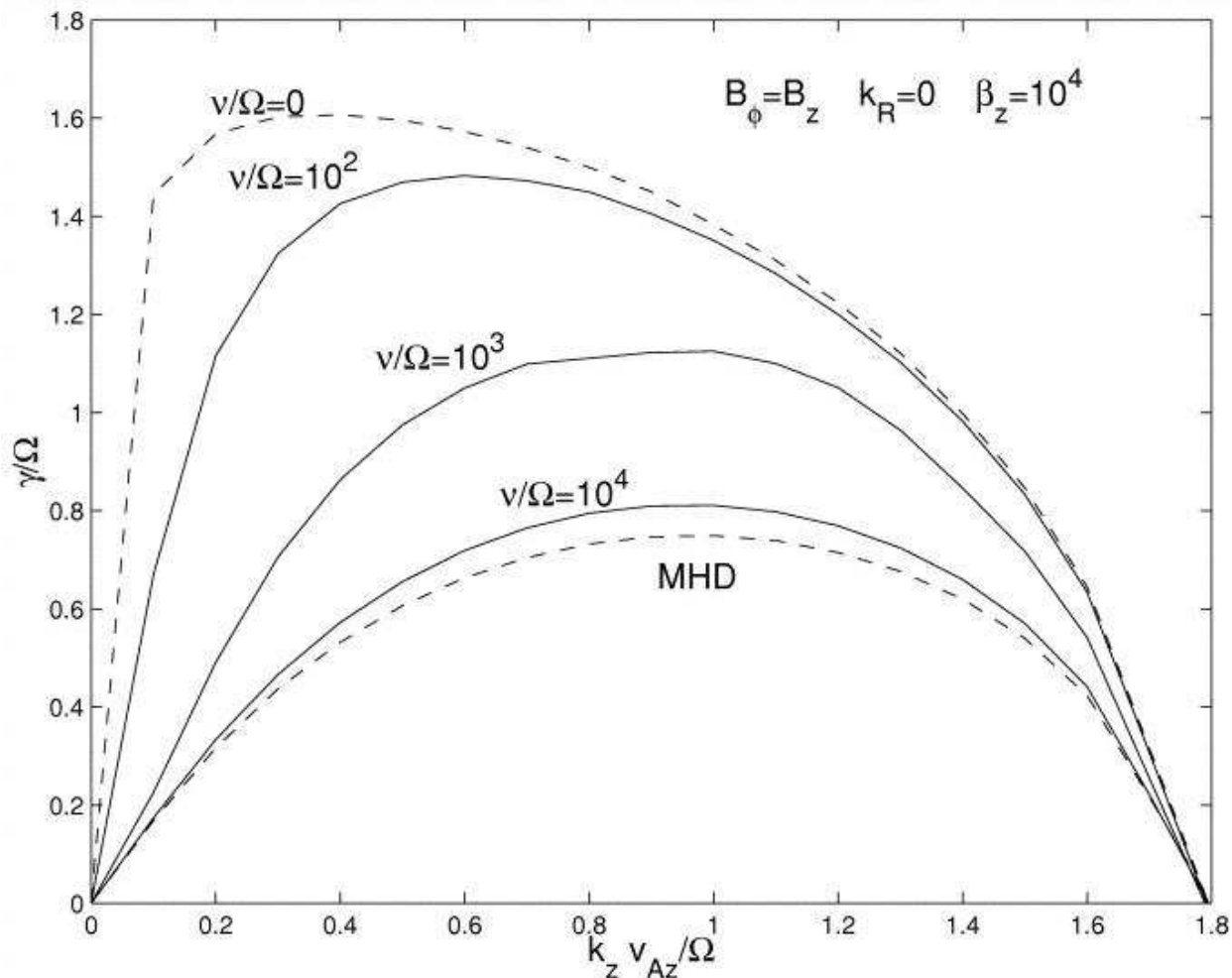


Fig. 3.— Dispersion relation for the magnetoviscous instability based on a kinetic treatment (figure adapted from Sharma et al. 2003).

an investigation combining both viscous and thermal effects is relatively straightforward via a fluid treatment; both effects need to be included in a study of high temperature accretion flows. This will be presented in a forthcoming paper by the authors.

It should be noted, however, that the effort entailed in a kinetic treatment has valuable dividends. It is difficult to know, for example, how far into the long mean free path regime an MHD fluid approach may be relied upon before collective instabilities might be triggered. This level of analysis can be provided only by a kinetic treatment (e.g., Schekochihin et al. 2005).

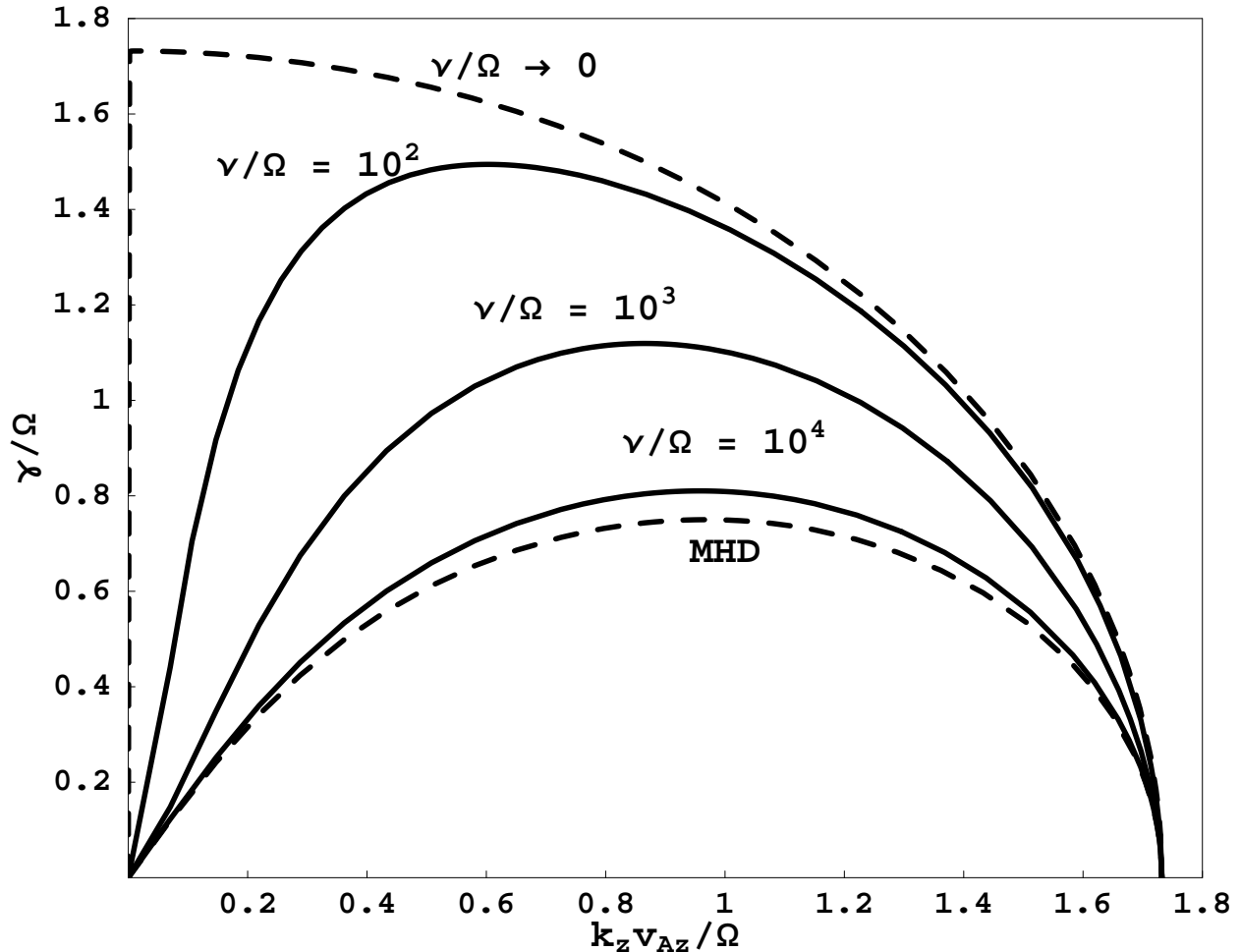


Fig. 4.— Dispersion relation for the magnetoviscous instability using an MHD fluid approach.

## 5. Conclusions

We have analyzed the stability of a dilute astrophysical plasma in the presence of Braginskii (1965) viscosity. Our main result is the dispersion relation (31). The regime of interest corresponds to gases in which the ion gyroradius is small compared to a mean free path. In laboratories this means a very strong field, but in astrophysical applications even very weak fields are in this regime when the density is sufficiently small. This regime does not apply to classical accretion disks or to stars (the densities are far too high), but it does apply to the interstellar medium of galaxies and protogalaxies, and to the low density accretion flows around some giant black holes (e.g. the Galactic center).

The work presented here extends the study of Balbus (2004), which included Braginskii viscosity but ignored  $\mathbf{J} \times \mathbf{B}$  Lorentz forces, and complements the plasma kinetic treatment of Sharma et al. (2003). The dynamical effects of the magnetic field lower the maximum growth rate found in the absence of such effects (eq. [34]), but growth rates significantly in excess of the MRI value  $0.5|d\Omega/d \ln R|$  are still found.

The magnetoviscous instability thus enhances the dynamo effect of the MRI in dilute gases, and therefore may well be a significant source of magnetic field amplification. Whether it is a more efficient mechanism than others that have been suggested (e.g. Schekochihin et al. 2004) is yet to be established, but numerical simulation of this large Prandtl number regime is clearly now a viable possibility. At the very least, MRI growth rates are significantly enhanced in the linear regime, and nonlinear field dissipation is inhibited (since the resistive scale is “blocked” in a downward cascade by dissipation at the larger viscous scale).

In the presence of strong temperature gradients in accretion flows, magnetothermal and magnetoviscous effects may both be important. Since a mere temperature gradient can now trigger convective instability, consequences for the temperature structure of inefficiently radiating accretion flows can in principle be profound. These will be discussed in a forthcoming paper.

### Acknowledgements

It is a pleasure to acknowledge useful discussions with S. Cowley, W. Dorland, and E. Quataert. We thank the anonymous referee for constructive comments leading to a greater clarity of presentation. This work was supported in part by the National Science Foundation under Grant No. PHY99-07949, and by NASA Grants NAG5-13288 and NNG04GK77G.

### REFERENCES

- Balbus, S. A. 2001, ApJ, 562, 909
- Balbus, S. A. 2004, ApJ, 616, 857
- Balbus, S. A., & Hawley, J. F. 1991, ApJ, 376, 214
- Balbus, S. A., & Hawley, J. F. 1998, Rev. Mod. Phys., 70, 1
- Biermann, L. 1950, Z. Naturforsch., 5a, 65

- Braginskii, S. I. 1965, *Reviews Plasma Physics*, New York: Consultants Bureau Enterprises, 1, 205
- Kulsrud, R. 1986, in *Plasma Astrophysics*, T. D. Guyenne & L. M. Zeleny, Paris: ESA Publ. SP-251, 531
- Chew, G. F., Goldberger, M., & Low, F. 1956, *Proc. Roy. Soc. London A*, 236, 112
- Melia, F., & Falcke, H. 2000, *ARA&A*, 39, 309
- Narayan, R., Mahadevan, R., & Quataert, E. 1998, in *Theory of Black Hole Accretion Disks*, eds. M. Abramowicz, G. Bjornsson, & J. E. Pringle (Cambridge: Cambridge University Press), 148
- Parrish, I., & Stone, J. 2005, *ApJ*, submitted
- Quataert, E., Dorland, W., & Hammett, G. W. 2002, *ApJ*, 577, 524
- Rees, M. J. 1993, in *Cosmical Magnetism*, D. Lynden-Bell, Dordrecht: Kluwer, 155
- Sharma, P., Hammett, G., Quataert, E. 2003, *ApJ* 596, 1121
- Schekochihin, A., Cowley, S. C., Kulsrud, R. M., Hammett, G. W., & Sharma, P. 2005, [astro-ph/0501362](#)
- Schekochihin, A., Cowley, S. C., Taylor, S. F., Maron, J. L., McWilliams, J. C. 2004, *ApJ*, 612, 276
- Snyder, P., Hammett, G., & Dorland, W. 1997, *Phys. Plasmas*, 4, 3974
- Spitzer, L., *Physics of Fully Ionized Gases*, New York: Wiley